Final Report

Crustal Deformation of the San Francisco Bay Area Segment of the San Andreas Fault from Persistent Scatterer InSAR

NEHRP Contract 06HQGR0056

Submitted by

Howard A. Zebker
Stanford University, Department of Geophysics
397 Panama Mall
Mitchell Bldg., Room 360, MC 2215
Stanford, CA 94306-2215
Tel: 650 723 8067, FAX 650 725 7344
zebker@stanford.edu

Research period: Jan. 1, 2006 – Dec. 31, 2006

Abstract

We report here a new InSAR persistent scatterer (PS) selection method based on a maximum likelihood information theoretic approach. This report summarizes work conducted under the NEHRP program from Jan. – Dec. 2006. Our method for identifying PS pixels in a series of interferograms is based on primarily comparing the phase characteristics of pixels with the theoretical distributions corresponding to assumed signal models. We have examined two signal models to describe the radar signals from resolution elements in SAR images statistically and derived their corresponding theoretical interferometric phase distributions, which we then use in the maximum likelihood estimation (MLE) process. Our method uses the description of persistent scattering described by Hooper et al. (2004), with appropriate changes made to the PS selection stage. Our method finds a dense network of scatterers with stable phase characteristics in areas where conventional InSAR fails due to complete decorrelation of the majority of scatterers, and in addition finds a denser network than is derived using previous PS methods. We compare our results with the method of Ferretti (2000) and Hooper et al. (2004) for two test regions in the San Francisco bay area, and find that we are able to identify PS pixels in previously uncorrelated regions. Thus our approach can define a network of deformation measurements in vegetated regions, as illustrated in the two test areas along the San Andreas Fault and Hayward Fault in the San Francisco Bay Area.

Background

Measurements of crustal deformation have contributed greatly to our understanding of

tectonics, earthquakes, volcanism, and landslides. Surface deformation measurements are used routinely to constrain the subsurface geometry of active faults and the spatial distribution of coseismic slip. Even more importantly, these data provide our primary means for recording aseismic processes such as afterslip, viscoelastic and poroelastic adjustments and so-called silent earthquakes. Geodetic measurements provide invaluable constraints on the interseismic accumulation of strain that will ultimately be released in large and damaging earthquakes. Volcanic eruptions, often preceded by the migration of large volumes of magma from the mantle through the crust, may be studied through the response of the elastic crust to the magma intrusion. We observe this through precise measurements of inflationary doming and stretching of the crust. Finally, deformation measurements play an important role in quantifying the kinematics of active landslides.

Despite the tremendous advances in both GPS and InSAR during the last decade, a major limitation in our ability to model these and other crustal processes is the lack of deformation data in many areas. While conventional InSAR is a proven, very effective technique for measuring deformation from active volcanism (e.g., Lu et al., 1998; Wicks et al., 1998; Pritchard and Simons, 2002), co- and post-seismic motions (e.g., Jonsson et al., 2002; Wright et al, 2001; Fialko, 2004), and ground subsidence from the withdrawal of groundwater (e.g., Hoffmann et al., 2001), almost any interferogram includes large areas where the signals "decorrelate" and no measurement is possible. If the surface is vegetated, weathers appreciably or is prone to snow coverage, the scattering properties change with time leading to a loss of interferometric coherence, a phenomenon known as "temporal decorrelation" (Li and Goldstein, 1990; Zebker and Villasenor, 1992). Consequently, most InSAR studies to date have focused on areas that are dry and sparsely vegetated, for example, in the desert southwest of the U.S., Turkey, or Tibet.

Decorrelation can also result from variations in imaging geometry. If the perpendicular baseline, the distance between the orbital tracks of the spacecraft at the two times scenes are acquired, is non-zero, the difference in incidence angle alters the coherent sum of wavelets from the many small scattering elements within a resolution cell (see below), so that measurements do not repeat exactly. This phenomenon, referred to as "spatial decorrelation" (Zebker and Villasenor, 1992), increases as the baseline increases. Thus, poor orbit control produces candidate InSAR pairs with excessive baselines that cannot be used to produce interferograms. Although this noise can be reduced by filtering, there are critical values of baseline and orbit control beyond which there is complete loss of interferogram coherence (Zebker and Villasenor, 1992).

In summary, even if copious SAR data are acquired, temporal and spatial decorrelation limit the usefulness of interferograms and remains the most significant shortcoming of InSAR. The new method we have demonstrated here under the NEHRP program will allow data from existing SAR satellites to be used to the maximum extent possible.

Advantages of Persistent Scatterer Methods. Both temporal and spatial decorrelation limit the use of conventional InSAR to mostly dry, sparsely vegetated areas, yet hazards are distributed globally. Six years ago Ferretti et al. (2000, 2001) proposed a new analysis method, denoted Permanent Scatterers in their patented procedure, to overcome

the decorrelation effects. In this approach resolution elements whose echo is dominated by a single scatterer are sought. If a resolution element contains only one scatterer, there is no cancellation of the echo as the imaging geometry varies, eliminating spatial decorrelation, nor is there temporal decorrelation due to the random motion of small scatterers over time. The method has since been enhanced and extended by Colesanti et al. (2003) and by us (Hooper et al., 2004); similar processing systems have been developed by various investigators (e.g., Adam et al., 2003; Crosetto et al., 2003; Lyons and Sandwell, 2003; Werner et al., 2003).

Conventional InSAR remains a very effective technique for measuring crustal deformation, but any interferogram includes large areas where the signals decorrelate and no measurement is possible. Ferretti's technique has been useful for analysis in urban areas, where angular structures produce efficient reflectors that dominate background scattering. However, man-made structures are absent from most of the Earth's surface. Furthermore, this technique requires, a priori, an approximate temporal model for the deformation. Characterizing the temporal pattern of deformation is commonly one of the aims of any study.

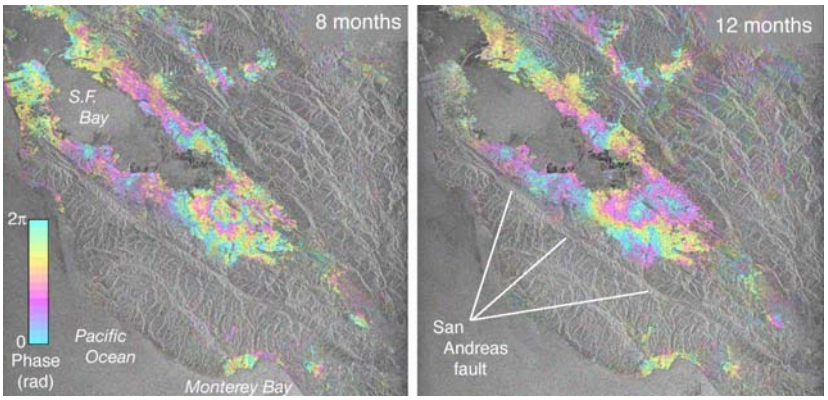

Fig. 1. 8-month (left) and 12-month (right) interferograms of the San Francisco Bay Area. Coherent phase signals are found only in urban areas, permitting some analysis of the Hayward fault along the eastern bay. No useful data are available for the San Andreas fault.

If we examine C-band (6-cm wavelength) interferograms from vegetated regions, we will very often find large areas of decorrelation. As an example, consider the northern California portion of the San Andreas fault. This region has so far resisted InSAR analysis, despite many satellite acquisitions over the area. The segment of the fault north of Monterey Bay, in particular, runs through terrain that is heavily vegetated and exhibits decorrelation in virtually all radar interferograms to date. Fig. 1 shows typical interferograms of the area, with 8-month (left) and 12-month time spans (right). Note that coherence is maintained only in the urbanized region around the Bay, allowing for useful analysis of data along the Hayward fault (Burgmann et al., 2000) but without any helpful measurements to the west of the San Andreas fault. Deformation estimates can be retrieved from interferograms only where the phase is coherent, which we recognize in phase images as regions where the measurement is correlated spatially. Typically, useful phase data correspond to correlation exceeding about 50%.

Higher correlation is seen in shorter-time interferograms, but cm-level noise from variations in atmospheric propagation necessitates time separations of a year or more to measure the at most several cm/yr expected deformations in this area. Thus, to date we have been unable to identify any possible slip across this fault segment from InSAR. As is often the case in similar areas of interest, the area is only sparsely covered by continuous GPS sites, further restricting our insight into its current deformation state. The most comprehensive network in the region, the Bard array, does span the fault in several spots but site spacing is 10's of km. While we could use these data in addition to InSAR to measure any deformation pattern, the wide spacing will not permit spatially detailed solutions of slip at depth. Several sets of campaign-style GPS data exist but these are sporadic in time. Hence, localized motions, and the ability to finely resolve any movement at depth from these data is limited. Large areas on the Earth have no network or campaign-style GPS data at all. Algorithms such as persistent scatter analysis may be the only way to observe detailed deformation patterns over many terrains.

Therefore, in this research we have tried to extend the persistent scatterer method to obtain as many reliable phase deformation points as possible in vegetated terrain. While some problems remain, we have increased the number of phase measurements significantly, opening the way for deformation analysis of many new regions on Earth.

What is a Persistent Scatterer? First, we define what is meant by the term persistent scatterer, and examine why only some points are "persistent." The degree of decorrelation in an InSAR image depends on the distribution of scattering centers within each resolution element, or "resel." In each resel the reflected wave is the coherent sum of individual wavelets scattered by many discrete scatterers (Fig. 2a). Constructive and destructive interference of these wavelets gives rise to amplitude scintillation (i.e., speckle). In contrast, if the resel is dominated by a single, very bright scatterer (Fig. 2c), only one wavelet is seen as there is little interference from other scatterers. The signal received from this resel is nearly invariant to imaging geometry, and any motion of the scatterer can be readily measured by the phase of the radar echo.

This is the model for a permanent scattering element. In between these extremes is a case where there is one larger scatterer among many smaller scatterers (Fig. 2b). Physically this might be a tree trunk dominating contributions from smaller branches and leaves, or a single large rock or facet amidst rubble. Here the received echo is the sum of one large term and many small terms, and depending on the ratio of the amplitudes of the large to the small scatterers the return can be very stable. Pixels with stable phase are our persistent scatterers (PS); with PS algorithms we try to identify and isolate these resolution elements.

The plot below the cartoons in Fig. 2 shows the results of radar echo simulations giving the phase of the radar echo if the individual scatterers move randomly between observations, in other words the effect of temporal decorrelation. This phase is equivalent to the phase seen in conventional radar interferograms; the amplitude of the pixel has a similar spread. Three cases are calculated: i) the dominant scatterer has an amplitude 10 times the smaller scattering points, ii) 3 times, and iii) equal amplitude to the surrounding

points. In case (iii), the phase is nearly random over the full +/-π interval. For case (i), the phase retrieved from the pixel is nearly constant over time. For the intermediate case, the phases are quite estimable, even though they do exhibit some scatter. Pixels with the characteristics of either (i) or (ii) form our persistent set.

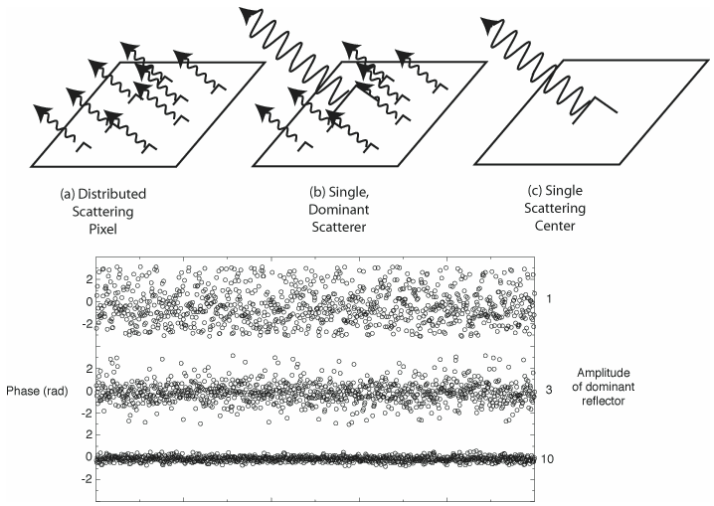

Fig. 2. Persistent scattering pixels and phase. In most naturally occurring resolution elements, the return is the coherent sum of many similar scatterers (a). Small changes in viewing geometry or random scatterer movement leads to baseline or temporal decorrelation, respectively. If a single bright scatterer is present (c), only one reflection is present and decorrelation disappears. Scatter plots at bottom show observed phase from a pixel containing a scatterer with amplitude of 1, 3, or 10 times the average background scatterer; phase from a resolution element with even 3 times the average background can be stable

Limitations of previous PS algorithms: Early PS systems, derived from Ferretti's initial work (2000), seek the pixels in an interferogram that are non-scintillating, or "permanent." An initial set of PS pixels that exhibit near-constant amplitude is identified, mainly those that are radar bright and truly dominated by a large scatterer. These are found by setting an empirical detection threshold on amplitude scintillation (Ferretti et al., 2001). This method works best in urban areas where man-made structures increase the likelihood of finding a non-fluctuating scatterer in any given pixel. With a few exceptions, the density of PS pixels identified by amplitude dispersion in natural terrains is generally too low to obtain reliable results.

Once an initial set of amplitude-stable scatterers has been identified, each candidate pixel phase is compared to nearby candidates. Only a point whose phase history is similar to the assumed model of deformation is deemed reliable and not merely the result of random chance. Reliable candidates are used to identify additional pixels using phase analysis. This approach can fail for two reasons.

First, the phase test involves wrapped phases and hence the noise term must be smaller than ±π. If the spatial distance between a reference PS and its neighbors is too large (usually ~2 km), the phase contribution from atmospheric delay can exceed ±π, and the pixel cannot be verified as persistent. A minimum PS density of 3-4 per km^2 is required (Colesanti et al., 2003). In most natural terrains, bright scatterers are rare and the density of reference PS is often too low to form a closely-spaced reference network. We find this holds for Long Valley caldera; it has also been noted for the central San

Andreas fault zone (Johanson and Bürgmann, 2001).

The second limitation is that temporal deformation must be known approximately because the data are wrapped, and the phase difference between the model and the actual deformation must be less than $\pm\pi$. As deformation is not usually known a priori, it is often assumed to be approximately constant in rate. If PS can be correctly identified, deviations from steady-state may be estimated from the residuals (Ferretti et al., 2000; Colesanti et al., 2003). This approach works as long as the deviations from steady state are small, as when deformation is due primarily to steady strain accumulation. In cases where deformation is episodic, including most volcanoes, landslides, or tectonic settings where the deformation is non-steady, such as post-seismic slip, a reliable network of reference PS can often not be identified.

Although PS have been identified on select volcanoes (e.g., Etna) and landslides (e.g., Berkeley Hills) where the deformation is to first-order steady-state, identifying stable scattering elements on other surfaces where the deformation is more complex has proven problematic (Hooper et al., 2004; Paolo Farina, pers. comm.). In order to be generally applicable, then, a PS method should produce a time series of deformation with no prior assumptions about its temporal nature. Hooper's method (2004), based on spatial correlation of phases rather than temporal consistency, does not require knowledge of the deformation history, thus is more robust for analysis of unknown deformation patterns.

However, even this method performs poorly over more heavily vegetated terrains such the in the San Francisco interferogram above (Fig. 1, also see Fig. 4 below). The main limitation is the paucity of identified PS points outside of the urban area, such as along the San Andreas fault segment shown here. Experiments with various threshold values in the initial PS selection have largely been unsuccessful in finding more, yet still reliable, points from which to form a deformation network.

We have since approached the selection problem using a more rigorous application of detection theory. Here we model the statistics of InSAR phase and apply a maximum likelihood test to each pixel to find points that match the expected phase distribution. This information theoretic approach finds many more PS points than the earlier algorithms and should enable a much wider range of terrains to be analyzed by InSAR.

Details of the new approach: maximum likelihood processing: Now we describe our new method for PS selection, discuss its use in phase unwrapping and filtering, and then summarize our approach to refine and apply PS to the most challenging deformation problems.

First, we model the radar echo from each observation of an interferometric pair as a correlated, complex Gaussian signal subject to additive Gaussian noise. The noise can result from either thermal noise sources, or from decorrelation as discussed in Zebker and Villasenor (1992). Following that paper, let $s_1 = c + n_1$ and $s_2 = c + n_2$ represent the signal return from a resolution element at two different times. n_1 and n_2 are complex Gaussian terms representing the sum of thermal noise plus the return from the weaker

scatterers in the resolution cell. The noise terms are uncorrelated with each other, as well as with *c*, itself complex Gaussian and which represents the return from the stronger scatterers in a resolution element. The probability distribution function of the measured interferometric phase (arg $s_1 s_2^*$) about a mean phase is (Just and Bamler, 1994)

$$p(\phi) = \frac{1-|\rho|^2}{2\pi} \cdot \frac{1}{1-|\rho|^2 \cos^2\phi} \cdot \left\{ 1 + \frac{|\rho| \cos\phi \arccos\left(-|\rho|\cos\phi\right)}{\sqrt{1-|\rho|^2 \cos^2\phi}} \right\} \qquad \text{Eq. (1)}$$

where the correlation ρ results from all sources of correlation. The distribution depends only on the correlation (or, equivalently, on SNR, through ρ=1/(1+1/SNR)) for the pixel. We plot examples of the theoretical distribution for different parameter ρ values in Fig. 3.

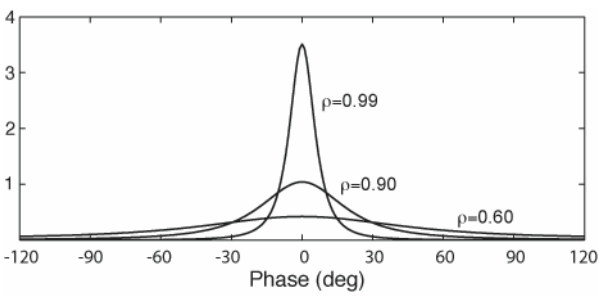

Fig. 3. Probability density function (pdf) of PS phase for several values of ρ. Maximum of observed pixel phase pdf conditioned on values of ρ for each pixel in an interferogram series determines whether we select that pixel as persistent.

Following Hooper et al. (2004), we express the residual phase, ϕ, of the *x*th pixel in the *i*th topographically corrected interferogram as the sum of 5 terms,

$$\phi_{x,i} = \phi_{def,x,i} + \phi_{\alpha,x,i} + \phi_{orb,x,i} + \phi_{\varepsilon,x,i} + n_{x,i} \qquad \text{Eq. (2)}$$

where ϕ_{def} is the phase change due to movement of the pixel (deformation) in the satellite line-of-sight (LOS) direction, ϕ_α is the difference in atmospheric delay between passes, ϕ_{orb} is the orbit error, ϕ_ε is the residual topographic error in the DEM and *n* is the "noise" term due to variability in scattering from the pixel, thermal noise and coregistration errors. We define pixels as PS if *n* follows the above ρ-parameterized distribution, and retain the PS for which the best estimate of ρ exceeds a threshold (see below).

Hooper et al. [2004] showed that all of the terms in Eq. (2) are either spatially correlated or correlated with the InSAR baseline, with the exception of the noise term. We estimate and remove these by filtering, and we are left with the noise term $n_{x,i}$. This noise term represents the combined phase contribution of the all of scatterers in the resolution cell plus actual system noises, and our test is to see if it matches the distributions above. The maximum likelihood method is to select the value of ρ for which the probability *P* conditioned on the measurements n_i

$$P(\rho \mid n_1, \cdots, n_k)$$

is maximized, where $P(A|B)$ refers to the conditional probability of event A with respect to event B. Using Bayes' rule,

$$P(\rho \mid n_1, \cdots, n_k) = \frac{P(n_1, \cdots, n_k \mid \rho) \cdot P(\rho)}{P(n_1, \cdots, n_k)} \qquad \text{Eq. (3)}$$

Noting that i) the denominator on the right hand side of Eq. (3) is independent of ρ, ii) in the absence of any knowledge of ρ for a given pixel we assume all values are equally likely, and iii) the noises are independent, we simply maximize the product

$$P(n_1 \mid \rho) \cdots P(n_k \mid \rho)$$

over all values of ρ. We then compare the estimated ρ to a threshold value, and if it exceeds the threshold we save that point as a PS. Our choice for a threshold follows the reasoning of Hooper et al. (2006), which yields a numerical value of 0.65 in this case. This ensures that we will find all of the PS pixels that Hooper finds, plus any of the dimmer pixels that are stable phase-wise. As seen in Fig. 4 below, many more points are found than with the existing algorithms.

As long as the density of PS is such that the corrected phase difference is generally less than π, the corrected phases can be unwrapped. The unwrapping problem here is in three dimensions (two spatial, and one temporal), for which no efficient algorithms have yet been developed. We have so far used a least-squares method (Hooper and Zebker, 2006) that worked fairly well on the Long Valley and Alcedo data sets, but may be inaccurate when applied to the images shown in Fig. 4.

A significant problem driving the unwrapping errors is that the spatial density of PS points in natural terrains may be too low to adequately represent a deformation network. Earlier work by Colesanti et al. (2003) suggested that a density of 3-4 PS/km^2 was sufficient to support a network, but this argument was based on analysis of Ferretti-type PS that were all very bright and dominated by man-made scattering objects. Our method can find much dimmer, and hence lower correlated and lower SNR PS, so the individual phases are noisier. This greatly increases the chances of phase unwrapping errors using simple algorithms.

We overcame this limitation in the 2-D unwrapping case by introducing statistical tests into the unwrapping procedure and formulating phase unwrapping as a network flow problem (Chen and Zebker, 2000; 2001). While Hooper's least-squares approach remains a viable starting point and can be expected to yield reliable results for some situations, we still need to improve the unwrapping algorithms so that we may apply the denser PS networks we find to deformation mapping in heavily vegetated areas.

After unwrapping, four other terms remain in Eq. (2) which mask ϕ_{def}. Unlike ϕ_{def}, we assume that the spatially correlated component of these error terms is uncorrelated temporally. Hooper used high-pass filtering of the unwrapped data in time, then low-pass filtering in space to resolve the spatially correlated error (similar to Ferretti et al., 2001). Subtracting this signal leaves only ϕ_{def} plus spatially uncorrelated terms that are the residual noise in our system. Given the success of maximum likelihood estimation for extracting PS scatterers from InSAR echoes, in future work we will replace these simple

filtering operations with information-theoretic algorithms, which should give much more reliable estimates of the deformation signal.

Results. We show the results of the new selection method (Fig. 4a,b) on the San Andreas and Hayward faults in the San Francisco Bay Area. Many more points are identified, especially in the rural terrains.

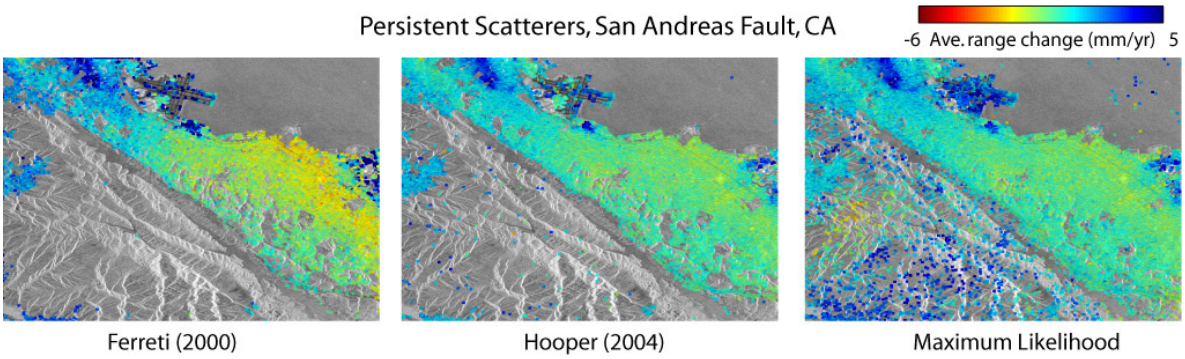

Fig. 4a. PS points identified using the methods of Ferretti (2000) and Hooper (2004), plus our information theoretic maximum likelihood algorithm. The ERS-1 and -2 time series was from 1992 to 2000. Only the maximum likelihood method finds many points southwest of the fault. It is likely that some of these are ambiguous from phase unwrapping errors. The yellow to red patch in the left part of the image halfway down is one very uncertain area. Still, points are locally coherent, and the selection results are not random.

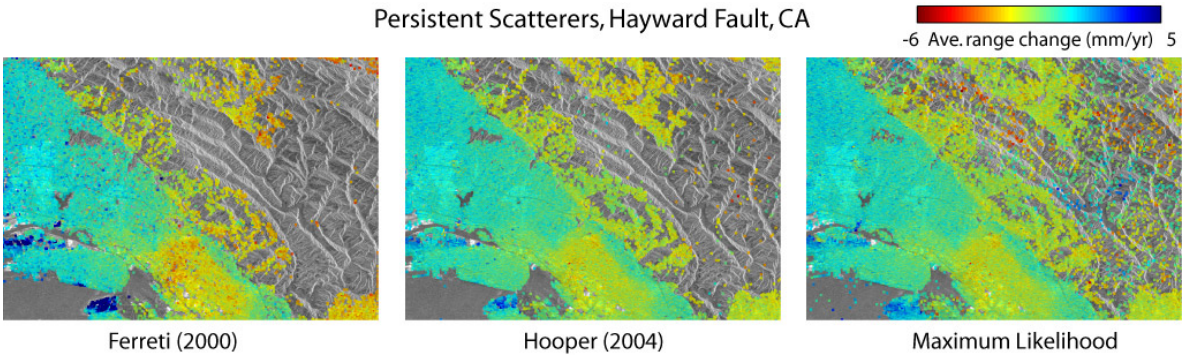

Fig. 4b. Similar analysis along Hayward fault. Slip along the fault is clear and agrees with observations of Burgmann et al. (2000). As above, phase unwrapping cautions apply.

While this method is highly promising for identifying many more PS points, it is also apparent from these images that the points in the sparser areas may be subject to phase unwrapping errors. The pixels are spatially coherent, though, showing that the additional points are in fact PS and not random selections. Examining the series of wrapped PS interferograms for the Hayward fault area (Fig. 5) clearly shows that coherence is high within any one image, so the variation seen in the interferograms of Fig. 4 is not random, it is either correct or else it suffers from phase unwrapping errors. Phase unwrapping remains an obstacle to unraveling the full deformation history.

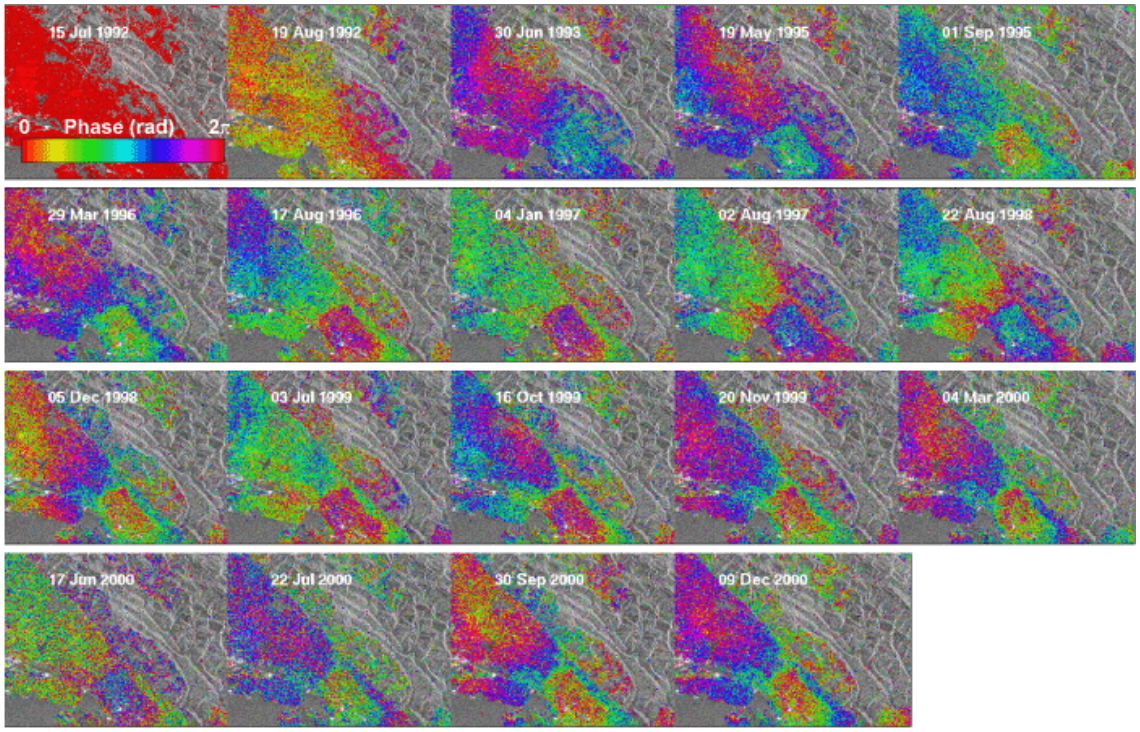

Fig. 5. Time series of PS interferograms of Hayward fault region. Coherence is high within the PS in any one image, so the variation seen in the cumulative interferograms of Fig. 4 is not random, either it is correct or else it suffers from phase unwrapping errors.

Summary

The new method for identifying persistent scattering pixels finds a much denser network of deformation measurements than is possible with either conventional InSAR or in existing algorithms for PS-InSAR. This advantage is particularly helpful in vegetated regions where the existing approaches have essentially failed repeatedly. While problems remain to be solved, especially that of phase unwrapping of the irregularly spaced and sparse data, we can now begin to analyze detailed crustal deformation in areas that have resisted crustal deformation modeling. Our results for the two faults we examined in the San Francisco Bay Area should permit deformation solutions in the near future.

References

Adam, N., B. Kampes, M. Eineder, J. Worawattanamateekul, and M. Kircher, The development of a scientific permanent scatterer system, *ISPRS Hannover Workshop Proceedings*, 2003.

Bamler, R. and D. Just, Phase statistics and decorrelation in SAR interferograms, *Geosci. and Remote Sens. Symposium, IGARSS '93*, 3, 980-984, 1993.

Bürgmann, R., D. Schmidt, R. M. Nadeau, M. d'Alessio, E. Fielding, D. Manaker, T. V. McEvilly, and M. H. Murray, Earthquake Potential Along the Northern Hayward Fault, California, *Science*, Vol 289, Issue 5482, pp. 1178-1182 , 18 August 2000.

Chen, C., and H. A. Zebker, “Network Approaches to Two-dimensional Phase Unwrapping: Intractability and Two New Algorithms,” J. Optical Society of America A, Vol. 17, No. 3, pp. 401-414, March, 2000.

Chen, C.W., Zebker, H.A., Two -dimensional phase unwrapping with use of statistical models for cost functions in nonlinear optimization, Journal of the Optical Society of America A (Optics, Image Science and Vision), Vol.18, No.2, p.338-51, Feb. 2001.

Colesanti, C., A. Ferretti, C. Prati, and F. Rocca, Monitoring landslides and tectonic motions with the permanent scatterers technique, *Eng. Geol*, 68 (1-2), 3-14, 2003.

Crosetto, M., A. Arnaud, J. Duro, E. Biescas, and M. Agudo, Deformation monitoring using remotely sensed radar interferometric data, *Proc., 11th FIG Symposium on Deformation Measurements, Santorini*, 2003.

Dehls, J. F., M. Basilico, and C. Colesanti, Ground deformation monitoring in the Ranafjord area of Norway by means of the permanent scatterers technique, *IEEE Int. Geosci and Remote Sensing Symposium. IGARSS 2002*, *1*, 203 - 207, 2002.

Ferretti, A., C. Prati, and F. Rocca, Nonlinear subsidence rate estimation using permanent scatterers in differential SAR interferometry, *IEEE Trans. on Geosci. and Remote Sensing*, *38*(5), 2202 - 2212, 2000.

Ferretti, A., C. Prati, and F. Rocca, Permanent scatterers in SAR interferometry, *IEEE Trans. on Geosci. and Remote Sensing*, *39*(1), 8 - 20, 2001.

Ferretti, A., F. Novali, R. Bürgmann, G. Hilley, and C. Prati, InSAR Permanent Scatterer Analysis Reveals Ups and Downs in the San Francisco Bay Area, *Eos*, 85 (34), 317, 324, 2004.

Fialko, Y., M. Simons, and Y. Khazan, Finite source modelling of magmatic unrest in Socorro, New Mexico, and Long Valley, california., *Geophys J. Int.*, *146*(1), 191 - 200, 2001.

Hilley, G. E., R. Burgmann, A. Ferretti, F. Novali, and F. Rocca, Dynamics of slow-moving landslides from permanent scatterer analysis, *Science* 25, v.304, no.5679, p.1952-5, 2004.

Hooper A., H. Zebker, P. Segall, and B. Kampes, A New Method for Measuring Deformation on Volcanoes and Other Natural Terrains Using InSAR Persistent Scatterers, *Geophys. Res. Lett.*, v.31, doi:10.1029/2004GL021737, 2004.

Hooper, A., P. Segall, and H. Zebker, Persistent Scatterer InSAR for Crustal Deformation Analysis, with Application to Volcán Alcedo, Galápagos, submitted to J. Geophys. Res., 2006.

Hooper, A., and H. Zebker, Phase Unwrapping in Three Dimensions with Application to InSAR Time Series, submitted to J. Optical Soc. of America, 2006.

Hooper, A., Ph.D. Thesis, Stanford University, Persistent Scatterer Radar Interferometry for Crustal Deformation Studies and Modeling of Volcanic Deformation, 2006.

Johanson, I.A., and R. Bürgmann, Using point measurements from InSAR to detect transient deformation, *EOS Trans.*, AGU, 82 (47), 266, 2001.

Jonsson, S., H. Zebker, P. Segall, and F. Amelung, Fault slip distribution of the 1999 Mw 7.1 Hector Mine, California, earthquake, estimated from satellite radar and GPS measurements, *Bull. Seis. Soc. Amer.*, vol.92, no.4, p.1377-89, 2002.

Just, D. and R. Bamler, Phase statistics of interferograms with applications to synthetic aperture RADAR, *App. Optics*, 33 (20), 4361-4368, 1994.

Lu, Z., D. Mann, and J. Freymueller, Satellite radar interferometry measures deformation

at Okmok volcano, *Eos Trans*., 79, 467-468, 1998.
Lu, Z., T. Wright, C. Wicks, Deformation of the 2002 Denali Fault Earthquakes, Mapped by Radarsat-1 Interferometry, *Eos*, Vol. 84, No. 41, 14, p 425, 430–431, 2003.
Lyons, S., and D. Sandwell, Fault creep along the southern San Andreas from interferometric synthetic aperture radar, permanent scatterers, and stacking, *J. Geophys. Res.*, *108*(B1), 2047 - 2070, 2003.
Owen, S.; Segall, P.; Freymueller, J.; Miklius, A.; Denlinger, R., Arnadottir, T.; Sako, M.; Burgmann, R., Rapid deformation of the south flank of Kilauea Volcano, Hawaii, Science, vol.267, no.5202, pp.1328-1332, 03 Mar 1995.
Owen, S., [Monograph] GPS measurements and kinematic models of the surface deformation on Kilauea Volcano, Hawaii, 152 pp., 1999a.
Owen, S.; Segall, P.l; Lisowski, M.; Miklius, A., Studying Kilauea Volcano's faults and rifts with GPS, International Union of Geodesy and Geophysics General Assembly, vol.99, Week B, pp.100, 1999b.
Pritchard, M. and M. Simons, A satellite geodetic survey of large-scale deformation of volcanic centres in the central Andes, *Nature*, 418, 167-171, 2002.
Thatcher W, and D. Massonnet, Crustal deformation at Long Valley Caldera, eastern California, 1992-1996 inferred from satellite radar interferometry. *Geophys. Res. Lett. 24*:2519-22, 1997.
Werner, C., U. Wegmüller, T. Strozzi, and A. Wiesmann, Interferometric point target analysis for deformation mapping, *Geosci. and Remote Sensing Symposium, IGARSS*, 2003.
Wicks, C., W. Thatcher, and D. Dzurisin, Migration of fluids beneath Yellowstone caldera inferred from satellite radar interferometry, *Science*, 282, 458-462, 1998.
Zebker, H. A., and J. Villasenor, Decorrelation in interferometric radar echoes., *IEEE Trans. on Geosci. and Remote Sensing*, *30*(5), 950 - 9, 1992.